# Synthesis of Magnetic Molecularly Imprinted Poly(ethylene-*co*-vinyl alcohol) Nanoparticles and Their Uses in the Extraction and Sensing of Target Molecules in Urine

**Mei-Hwa Lee,[†] James L. Thomas,[‡] Min-Hsien Ho,[§] Ching Yuan,[||] and Hung-Yin Lin*[,§]**

Department of Materials Science and Engineering, I-Shou University, Kaohsiung 840, Taiwan, Department of Physics and Astronomy, University of New Mexico, Albuquerque, New Mexico 87131, and Department of Chemical and Materials Engineering and Department of Civil and Environmental Engineering, National University of Kaohsiung, Kaohsiung 81148, Taiwan

**ABSTRACT** Superparamagnetic nanoparticles are of great current interest for biomedical applications in both diagnostics and treatment. Magnetic nanoparticles (MNP) can be manipulated by magnetic fields, so that when functionalized, they can be used for the purification and separation of biomolecules and even whole cells. Here we report combining the separation capabilities of MNPs with the functional (binding) capability of molecularly imprinted polymers. Albumin- creatinine-, lysozyme-, and urea-imprinted polymer nanoparticles were synthesized from poly(ethylene-*co*-ethylene alcohol) via phase inversion, with both target molecules and hydrophobic magnetic nanoparticles mixed within the polymer solution. Several ethylene:ethylene alcohol mole ratios were studied. The rebinding capacities for those three target molecules varied from 0.76 ± 0.02 to 5.97 ± 0.04 mg/g of molecularly imprinted magnetic nanoparticles. Lastly, the composite nanoparticles were used for separation and sensing of template molecules (e.g., human serum albumin) in real samples (urine) and results were compared with a commercial ARCHITECT *ci* 8200 system.

**KEYWORDS:** magnetic nanoparticles • poly(ethylene-*co*-ethylene alcohol) • creatinine • albumin • lysozyme • urea • molecular imprinting • urine

## 1. INTRODUCTION

The application of superparamagnetic iron oxide nanoparticles (SPIONs) to biomedical applications has received much interest recently; different approaches to their synthesis and surface engineering have been reviewed by Gupta and Gupta (1). Controlling interactions between living cells and SPIONs can be employed for (a) diagnosis, e.g. biosensing, magnetic resonance imaging (MRI) (2) and stem cell tracking; (b) separations, e.g., cell isolation or cellular proteomics; (c) therapies, e.g., hyperthermia, magnetofection, and drug delivery. The size of magnetic nanoparticles (MNPs) depends on their synthesis process. Precipitation from microemulsions, surfactant or polymer solutions can readily form nanoparticles with diameters <100 nm, giving superparamagnetic properties. Several biocompatible polymers have been coated on the MNP surface to enhance biocompatibility, including chitosan, dextran (2), poly(acrylic acid), polyethylene glycol, polylactide, polyvinyl alcohol, and phosphorycholine.

Proteins, peptides and folic acid have been applied for the targeting of MNPs, generally by conjugating these molecules to a polymeric MNP coating. However, the coating of biocompatible polymers and the conjugation of biomolecular ligands are time-consuming processes, and the final products may not exhibit long-term stability. Recently, molecular imprinting has been used to modify the surfaces of magnetic nanoparticles. Molecularly imprinted polymers (MIPs) have been extensively investigated because of their biomedical applications in biosensing (3) with optical (4), electrochemical (5), or QCM transducers (5); in bioseparation (6), especially for solid phase extraction or when packed in a chromatography column (7); and in drug delivery (8), when they have high affinity with the target bioactive molecules and thus release those molecules slowly (9). A decade ago, Ansell and Mosbach were the first to prepare magnetic molecularly imprinted polymers (MMIPs) via the suspension polymerization of poly(MAA-*co*-TRIM) to *(S)*-propranolol in a magnetic field (10). A similar approach was recently employed to synthesize MMIPs to remove amino acids (e.g., tryptophan (11), tyrosine, and phenylanine (12)), atrazine (13), cadmium (14), and tetracycline antibiotics (6c). Other biomaterial, such as chitosan, has been utilized to prepare magnetic Cu(II)-imprinted chitosan composites for the selective removal of copper ion (15). A molecularly imprinted polymer-

* To whom correspondence should be addressed: Department of Chemical and Materials Engineering, National University of Kaohsiung (NUK), 700, Kaohsiung University Rd., Nan-Tzu District, Kaohsiung 811, Taiwan, Tel: (O) +886(7)591-9455; (M) +886(912)178-751, E-Mail: (H.-Y. Lin): linhy@ntu.edu.tw or linhy@caa.columbia.edu.

Received for review March 16, 2010 and accepted May 24, 2010

[†] I-Shou University.

[‡] University of New Mexico.

[§] Department of Chemical and Materials Engineering, National University of Kaohsiung.

[||] Department of Civil and Environmental Engineering, National University of Kaohsiung.

DOI: 10.1021/am100227r

coated nanocomposite containing magnetic nanoparticles was synthesized using the sol–gel method with TEOS to form $Fe_3O_4$@$SiO_2$ MNPs, which then reacted with a template–silica monomer complex to produce estrone-imprinted MNPs (16).

Poly(ethylene-*co*-vinyl alcohols) (EVALs) have a porous microstructure that is stable under ultrafiltration (17), and their specific adsorption properties also show potential for clinical application (18). In the authors' earlier investigations, poly(ethylene-co-vinyl alcohols) (EVALs) with various ethylene contents were adopted as the imprinted polymers (19), and biomarkers in urine were selected as the target molecules. Random urine samples were tested to determine whether interferences from realistic 'contaminants' affect the recognition and quantification capabilites of molecularly imprinted polymers. Urine contains nonprotein nitrogen metabolites, carbohydrates and proteins, in concentrations of less than 0.6–10 mg/mL, 44–500 $\mu$g/mL, and 0.1–20 $\mu$g/mL, respectively. The high concentration of nonprotein nitrogen metabolites such as urea can saturate the cavities on the surface of molecularly imprinted polymers. Hence, the selective removal of molecules (such as urea) from urine may beneficially reduce the interference effect. Also, the active binding of target molecules on magnetic molecularly imprinted polymers selectively separates clinically valuable target molecules (such as proteins) from the biological fluids.

In this work, some biomarkers in urine, including urea, creatinine, albumin, and lysozyme were employed as template molecules during the polymeric processing by phase inversion separation to imprint these target molecules on the EVAL. Before the precipitation process, hydrophobic magnetic nanoparticles were premixed within EVAL/DMSO solutions. After particle formation, the template molecules were removed by washing with SDS solution on a magnetic plate. Experimental results demonstrate that the magnetic molecularly imprinted EVALs are selective toward the target molecules. The magnetic molecularly imprinted composite nanoparticles can also be utilized as signaling labels, through the measurement of magnetic flux after they have been incubated with different concentrations of the target. Comparison of measurements of real urine samples with results from a commercial analysis system (Architect *ci* 8200) indicates that the MMIPs have sensing potential, but that future work is needed to quantify the roles of interferences from nontarget proteins.

## 2. EXPERIMENTAL SECTION

**2.1. Reagents.** Creatinine, albumin (from bovine serum, minimum 98%), lysozyme (from hen egg white), and poly(ethylene-*co*vinyl alcohol), EVAL, with ethylene 27, 32, 38, and 44 mol % (product no. 414077, 414093, 414085, 414107) were from Sigma-Aldrich Co. (St. Louis, MO). Urea was from Acros Organics (Geel, Belgium). Dimethyl sulfoxide (DMSO, product # 161954) was purchased from Panreac (Barcelona, Spain) and used as the solvent to dissolve EVAL polymer particles in the concentration of 1 wt %. Iron(III) chloride 6-hydrate (97%) and iron(II) sulfate 7-hydrate (99.0%) were also from Panreac. Absolute ethyl alcohol was from J. T. Baker (ACS grade, NJ). Sodium dodecyl sulfate (SDS) were purchased from Sigma-Aldrich Co. (St. Louis, MO) and used for the removal of target molecules. All chemicals were used as received unless otherwise mentioned.

**Scheme 1. Separation of Target Molecules Using MMIP Nanoparticles in Urine**

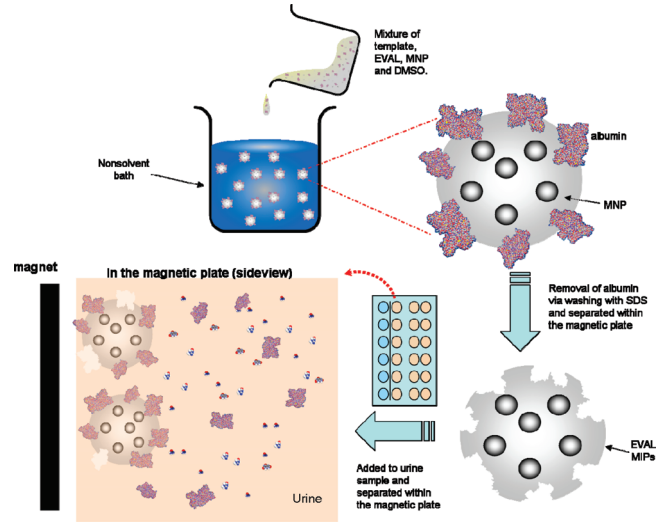


**2.2. Formation of Magnetic Molecularly Imprinted Poly(ethylene-*co*-ethylene alcohol) Composite Nanoparticles.** The synthesis of magnetic albumin-imprinted, lysozyme-imprinted, creatinine- imprinted and nonimprinted EVAL nanoparticles included four steps (as shown in Scheme 1). (a) Magnetic nanoparticles were synthesized by the Massart method, which is simply coprecipitation of a mixture of iron(III) chloride 6-hydrate and iron(II) sulfate 7-hydrate by sodium hydroxide. This magnetite was mixed with oleic acid for better dispersion and repeatedly washed while adsorbed on a magnetic plate, and then freeze-dried overnight. (b) Dried magnetic nanoparticles were added to the EVAL solution (EVAL/DMSO = 1 wt %) to a concentration of 20 mg/mL. The EVAL/magnetic particle solution was mixed with 0.03, 0.1, or 0.5 wt % of templates creatinine, albumin or lysozyme. Although proteins may denatured by DMSO, it is often still possible to obtain good recognition; it appears likely that small structural fragments of a protein are the actual recognition elements in these MIPs (20). The molecular recognition of small structural fragments is well established in immunology, where it is known epitopic recognition (21). (c) The EVAL/magnetic particle solution was dispersed into 10 mL nonsolvent solution (22) (deionized water/isopropanol = 2/3 in weight) for EVAL at 5 °C. (d) Template molecules were removed by washing with 2 mL 1 wt % SDS solution (for albumin and lysozyme) 10 min for two times and then deionized water 10 min for four times, using a magnetic plate to separate the MMIPs. With noncovalent MIPs, there is always the concern that the washing out of template could damage recognition sites. However, organic solvents (e.g., isopropanol) have been successfully used for the extraction of phospholipids from EVAL MIPs (23), so perisistance of recognition capability after washing is possible. (Imprinting effectiveness factors of ~6, reported herein and with the noncovalent phospholipids-recognizing MIPs noted above, require a difference of only ~2 $k_BT$ in binding energy between targets and nontargets.) The anionic SDS detergent is effective at protein template removal, as it disrupts hydrophobic bonding; as some recognition capability remains in the EVAL after this treatment, we conclude that nonhydrophobic interactions (such as hydrogen bonding) contribute to the stability of the precipitated EVAL.

All composite nanoparticles were equilibrated with deionized water overnight before use. The nonimprinted polymers (NIPs) were prepared identically, except that the template was omitted.

**2.3. Adsorption of the Templates to Magnetic MIP and NIP Composite Nanoparticles.** The rebinding of the template molecules or proteins (human albumin and lysozyme) to the molecularly imprinted or nonimprinted polymers were measured with 1 mL solutions of 0.02, 0.75, 0.002, and 5.0 mg/mL albumin, creatinine, lysozyme, and urea, which were dissolved in the phosphate buffer saline (PBS). These solutions were added to 1 mL of polymer particles (15 mg) in deionized water on a magnetic plate for 1 min. A UV/vis spectrophotometer (Lambda 40, PerkinElmer, Wellesley MA) was then used to measure the concentration decrease in the stock solution, determined by absorption at 235 nm for creatinine, 280 nm for albumin and lysozyme.

**2.4. Size Distribution and Zeta Potential of MIP Nanoparticles.** Creatinine-, albumin-, lysozyme-imprinted polymers and magnetic nanoparticles were monitored by a particle sizer (90Plus, Brookhaven Instruments Co., New York). The measurement of the particle size distribution was based on dynamic light scattering (DLS) at 25 °C with 3 min duration data collection at the 90° detection angle. The average count rate of the background was 15 kcps and that of each measurement was between 20 and 500 kcps. The scattering laser power of this instrument is the standard 35 mW. The CONTIN algorithm was used to analyze data.

**2.5. Surface Morphology Examination by Scanning Tunneling Microscopy and Atomic Force Microscopy.** Magnetic nanoparticles were synthesized as in section 2.2, coated with oleic acid and then freeze-dried before examination by a scanning tunneling microscope (easyScan 2, *Nanosurf* AG, Switzerland). The image size, scan speed, and points/line were $25 \times 25$ nm$^2$, 0.2 s/line, and 128, respectively, and the tip voltage was 50 mV.

**2.6. X-ray Diffraction Analysis of Magnetic Molecularly Imprinted Polymer Composite Particles.** X-ray diffraction analysis (D8 Advance XRD, Bruker, German) was used to determine the crystalline structure of the $\varepsilon$-$Fe_2O_3$ encapsulated MIP nanoparticles with Cu K$\alpha$ radiation $\lambda = 1.5406$ Å.

**2.7. Magnetization Measurement of Adsorption of Albumin Molecules on the Magnetic Molecularly Imprinted EVAL Composite Nanoparticles.** Superconducting quantum interference devices (SQUID) are very sensitive magnetometers used to measure extremely small magnetic fields, based on superconducting loops containing Josephson junctions. The magnetic nanoparticles, albumin-imprinted magnetic EVAL composite nanoparticles before and after removal of template were freeze-dried and their magnetization monitored with a the magnetic property measurement system (MPMS XL-7, Quantum Design, San Diego, CA) at 298 K in ±15000 G. Various concentrations of albumin were then added to the stock magnetic EVAL MIP nanoparticles 15 mg in 2 mL of PBS to plot the calibration curves. Random urine samples were secreted by our colleagues 4 h before the test. Each nanoparticle solution contained 2 $\mu$L of the stock urine sample and 2 mL of PBS mixture on a magnetic plate (as shown in Scheme 1). Samples were transferred to the wells in a magnetic field after 1 min stationary and extracted solution was removed after 10 min. The magnetic EVAL MIP nanoparticles were washed gently with DI water and then freeze-dried for the measurement of magnetization by SQUID. One milliliter of the urine sample was also stored in an eppendorf microcentrifuge tube at 4 °C and analyzed with ARCHITECT *ci* 8200 system (Abbott Laboratories. Abbott Park, Illinois, U.S.A.).

## 3. RESULTS AND DISCUSSION

The use of molecularly imprinted polymers as antibody mimics was originally developed for ligand-binding assays. Much attention has recently been paid to the incorporation of magnetic nanoparticles into molecularly imprinted polymers to separate target biomolecules from complex fluid mixtures. The approach of suspension polymerization was first applied a decade ago for preparing molecularly imprinted polymeric particles (10), giving particle sizes from approximately a few micrometers down to several hundred nanometers. The proportions or species of cross-linkers and functional monomers in molecularly imprinted polymers can be chosen to form a pseudostable emulsion during polymerization, and to control the final particle size via the emulsion droplet size. Larger particles work better in chromatography columns, as they do not collapse or block the flow, while smaller particles have higher specific surface areas, increasing the capacity of the molecularly imprinted polymer to absorb the target molecules. Conventional column chromatography results in dilution of the analyte during elution from the column. A potential advantage of magnetic MIPs is that they can in principle give higher final analyte concentrations, because the separation of the analyte and the particles can be achieved by magnetic fields, rather than by flow.

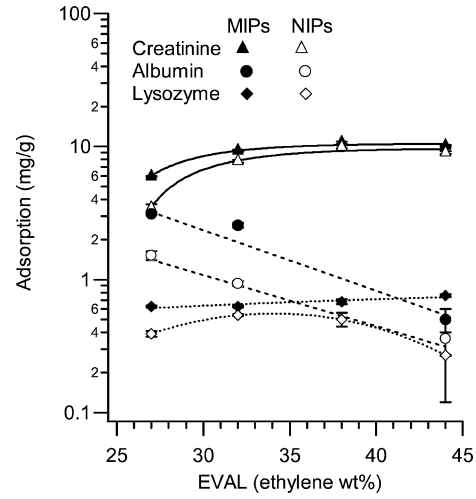


**FIGURE 1. Adsorption capacities of creatinine-, albumin-, lysozyme-, and non-imprinted EVAL polymer nanoparticles with different mole % of ethylene contents.**

Figure 1 presents the rebinding of the target molecules to the imprinted EVAL nanoparticles, as determined by the depletion of the target from the binding solution during a one-minute binding period. The adsorption of target molecules, including creatinine, albumin and lysozyme, by magnetic molecularly imprinted polymers is 1.73−2.77 times higher than of magnetic nonimprinted polymers, as presented in Table 1. The imprinting effectiveness (the ratio of binding on MIPs to binding on NIPs) is maximized for creatinine, albumin, and lysozyme when EVAL is employed with 27, 32, and 44 mol % of ethylene, respectively. These optimized ethylene ratios of EVALs were then utilized to further investigate the removal of target molecules from urine. Note that the imprinting effectiveness may be higher for MIPs if incubation with the target is allowed to proceed for a longer time. In particular, with albumin-imprinted (32 mol % ethylene) EVAL MMIPs, after a half-hour of stationary adsorption the imprinting effectiveness rose to ca. 6.15, vide infra. It is also interesting to note that the total rebinding

**Table 1. Rebinding of Template Molecules to the Magnetic Molecularly Imprinted and Nonimprinted Poly(ethylene-*co*-ethylene alcohol) and the Imprinting Effectiveness with Different Ethylene Mole %[a]**

| | creatinine adsorption (mg/g) | | | albumin adsorption (mg/g) | | | lysozyme adsorption (mg/g) | | |
|---|---|---|---|---|---|---|---|---|---|
| EVAL (ethylene mole%) | MMIP | MNIP | IF | MMIP | MNIP | IF | MMIP | MNIP | IF |
| **27** | **5.97 ± 0.04** | **3.46 ± 0.24** | **1.73** | 3.13 ± 0.06 | 1.52 ± 0.12 | 2.06 | 0.63 ± 0.01 | 0.39 ± 0.02 | 1.69 |
| **32** | 9.30 ± 0.18 | 7.74 ± 0.20 | 1.20 | **2.57 ± 0.10** | **0.93 ± 0.04** | **2.77** | 0.63 ± 0.01 | 0.54 ± 0.008 | 1.15 |
| 38 | 10.69 ± 0.22 | 9.96 ± 0.26 | 1.10 | 2.52 ± 0.02 | 1.97 ± 0.07 | 1.28 | 0.68 ± 0.03 | 0.50 ± 0.06 | 1.59 |
| **44** | 10.07 ± 0.20 | 9.00 ± 0.19 | 1.12 | 0.50 ± 0.10 | 0.36 ± 0.24 | 1.40 | **0.76 ± 0.02** | **0.27 ± 0.003** | **2.74** |

[a] MMIP, magnetic molecular imprinting polymer; MNIP, magnetic non-imprinting polymer; IF, imprinting effectiveness.

capacity (mg/g) for creatinine increased with increasing ethylene, while rebinding capacity for albumin decreased. For lysozyme, the binding to imprinted polymers increased slightly with increasing ethylene, but the nonspecific binding to nonimprinted polymer particles decreased, giving the highest effectiveness at highest ethylene mol %. These differences highlight the fact that the optimal composition for specific vs nonspecific binding may be quite different. An important consideration for specific binding will undoubtedly be the ability of the polymeric material to form complementary cavities to the target, whereas nonspecific binding will be dominated by interactions of individual chemical groups on the polymer and the target.

The adsorption dynamics of albumin MMIPs is presented in Figure 2a for the same adsorption condition in Figure 1. The adsorption reached equilibrium after 30 min and the maximum imprinting effectiveness reached 6.15 with a total capacity of 7.2 ± 0.55 mg/g. This result (for imprinting effectiveness) is as good as that obtained previously using various combinations of functional and cross-linking monomers (20).

The adsorption isotherm for 30 min adsorption is shown in Figure 2b. A number of different models have been applied to MIP binding isotherms, including Langmuir, Freundlich (24) and Langmuir–Freundlich isotherm (25) (reviewed by García-Calzón and Díaz-García (26).) A Freundlich isotherm, arising from a broad distribution of binding site affinities, did not fit the observed data well. We instead allowed for a Gaussian distribution of binding site affinities, fitting (using MatLab) for the mean dissociation constant, standard deviation of the dissociation constants, and the total capacity. The best fit three-parameter curve (shown in Figure 2b) gives a mean dissociation constant of 26.4 mg/L (394 nM), a saturation of 9.1 mg/g, and a remarkably narrow range of dissociation constants (<1 nM). This extremely narrow range of dissociation constants may indicate that only one "epitope" in albumin is effective as an imprinting target (at least within the concentration range studied.)

Figure 3a shows the morphology of the magnetic particles that were synthesized in this study. The surfaces of those magnetic nanoparticles are modified with oleic acid to aid in dispersion. The individual particles have sizes around 6–7 nm. Figure 3b shows the X-ray diffraction (XRD) patterns of $\varepsilon$-$Fe_2O_3$-encapsulated EVAL nanoparticles that were synthesized with imprinting with three target molecules - creatinine, albumin, and lysozyme. The X-ray diffraction peaks of the three samples correspond to (420), (411), and (031),

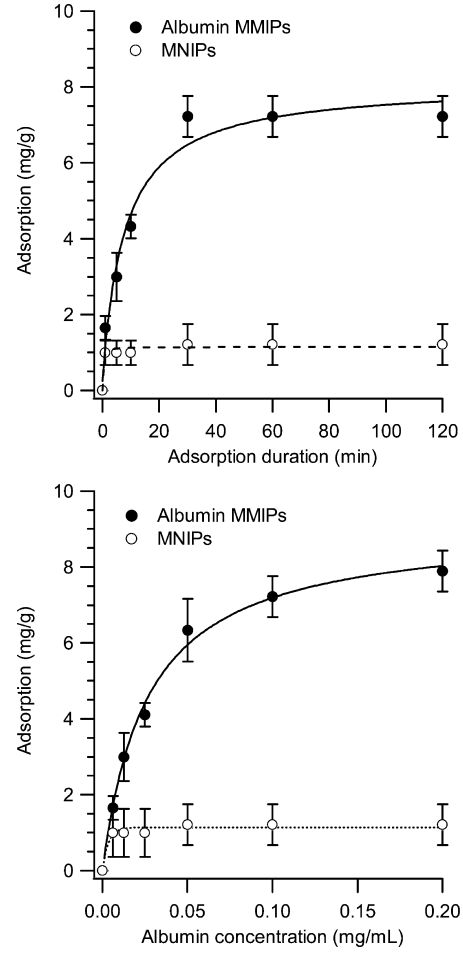


**FIGURE 2. (a) Binding of albumin vs time for magnetic MIPs. (b) Binding isotherm for different albumin concentrations.**

revealing that $\varepsilon$-$Fe_2O_3$ encapsulated in EVAL nanoparticles had a monoclinic structure (JCPDS card no. 16–0653).

Figure 4a plots the size distribution of molecularly imprinted EVAL particles, measured directly by dynamic light scattering. The size distribution of the magnetic nanoparticles is in the range 25–50 nm; these particles are larger than observed in the STM images in Figure 3a, suggesting that some aggregation had occurred in the light scattering preparation. The sizes of the creatinine-imprinted magnetic EVAL polymers, following the removal of creatinine, are close to those of the magnetic particles, as measured by DLS. Although the unwashed (presumably template-bound) lysozyme-imprinted magnetic EVAL particles are on average considerably larger than the albumin- and creatinine-imprinted magnetic EVAL nanoparticles, after SDS washing,

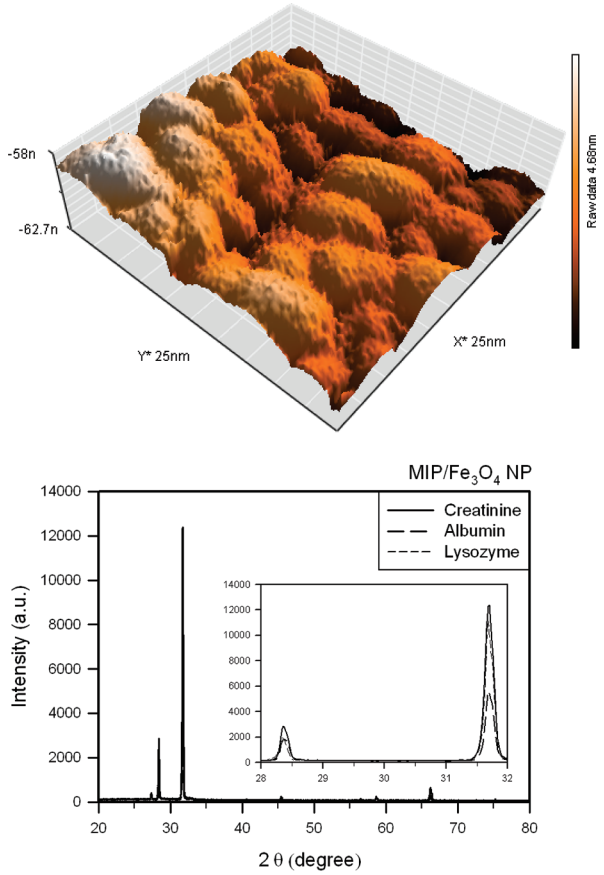


**FIGURE 3. (a) Scanning tunneling microscopic (STM) image of magnetic nanoparticles and (b) X-ray diffraction (XRD) pattern of the magnetic molecularly imprinted polymers.**

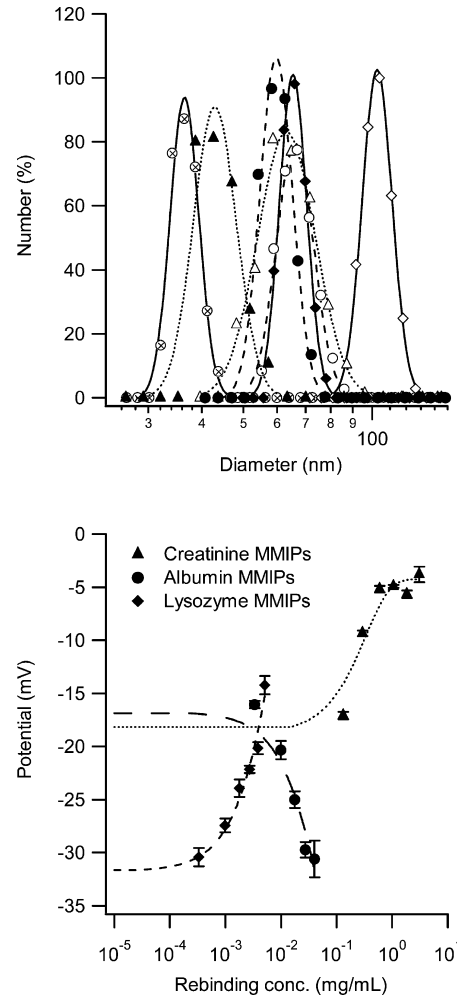


**FIGURE 4. The particles size distribution of (a) magnetic nanoparticles (⊕) and creatinine- (▲), albumin- (●), and lysozyme- (◆) imprinted magnetic EVAL particles before (empty) and after (filled) the washing. (b) The zeta potentials of creatinine-, albumin-, and lysozyme-imprinted EVAL polymeric nanoparticles titrated with target molecules at the reference concentrations.**

these particles become much smaller (Table 2). The differences in particle sizes here may be caused by the different ethylene mole percentages used, as well as differences in the physicochemical interactions among the polymer, the template, and the magnetic nanoparticle. The mean particles sizes for nonimprinting EVALs are 95 ± 4, 118 ± 5, 135 ± 4, and 149 ± 6 nm with 27, 32, 38, and 44 mol % ethylene. Interestingly, the reduction in the mean size of albumin-imprinted magnetic EVAL nanoparticles on washing is only about 6 nm. This likely reflects a lower level of template incorporation into the MIP, but could also be caused by greater retention of this template, compared with creatinine or lysozyme. Table 2 also presents the zeta-potentials of these magnetic molecularly imprinted nanoparticles. The surface charges on the creatinine- and lysozyme-imprinted magnetic EVAL nanoparticles are reduced, and the surface charge on the lysoyme-imprinted magnetic nanoparticles is about half that on creatinine- and albumin-imprinted magnetic EVAL nanoparticles. The surface charges on creatinine- and albumin-imprinted magnetic EVAL nanoparticles are −17.49 ± 0.38 and −19.06 ± 0.43 mV, respectively. Figure 4b presents the titration of target molecules against the magnetic molecularly imprinted EVAL nanoparticles. The (negative) surface charge of the creatinine- and lysozyme-imprinted magnetic EVAL nanoparticles decreased with the concentration of the target molecules; the surfaces became more neutral (approaching complete neutrality for creatinine MIPs).

**Table 2. Mean Particle Sizes and Zeta-Potentials of Magnetic Molecularly Imprinted Polymers**

| MMIPs | | particle size (nm) | | zeta potential (mV) | |
|---|---|---|---|---|---|
| template | EVAL (ethylene mole %) | before washing | after washing | before washing | after washing |
| creatinine | 27 | 64 ± 8 | 44 ± 3 | −1.35 ± 1.83 | −17.49 ± 0.38 |
| albumin | 32 | 67 ± 4 | 61 ± 5 | −31.63 ± 0.51 | −19.06 ± 0.43 |
| lysozyme | 44 | 107 ± 4 | 66 ± 4 | 4.32 ± 1.22 | −32.13 ± 1.09 |

Figure 5 depicts the magnetization of the magnetic MIPs, caused by an external magnetic field fielding the range of ±15000 G. Changes in magnetizability may depend on the size and aggregatability of the MIP nanoparticles. The magnetizations of the magnetic nanoparticles, and of magnetic albumin-imprinted nanoparticles (after template removal), are both 17.3−18.4 emu/g in a field of 15 000 G. These magnetization values can depend on the synthesis methods (1). The magnetic molecularly imprinted nanoparticles be-

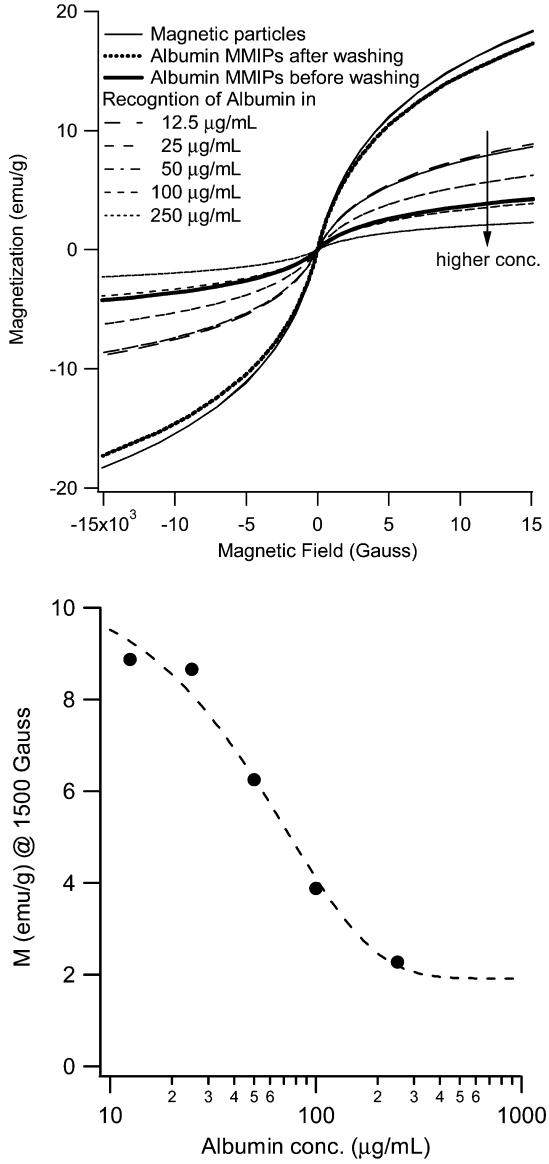


**FIGURE 5. (a) Superconducting quantum interference devices (SQUIDs) magnetization measurement of albumin-imprinted magnetic EVAL nanoparticles before and after the removal of template molecules, and after binding different concentrations of albumin. (b) The calibration curve of magnetization with different concentrations of albumin at an applied magnetic field of 15 000 G.**

fore the removal of albumin have a much smaller magnetization of around 4.26 emu/g in a field of 15 000 G. Chen et al. also observed a similar decrease in magnetizability when preparing magnetic molecularly imprinted polymers (6c). Moreover, the magnetization of the composite nanoparticles also decreased with increasing weight ratio of dextran to magnetite (2). Magnetization curves were obtained at concentrations of albumin of 12.5−250 $\mu$g/mL, absorbed by albumin-imprinted magnetic EVAL particles; increasing albumin concentration (and presumably absorption) monotonically reduces the magnetizability of the magnetic MIPs. Thus, magnetizability is a suitable readout mechanism for quantification of template binding. Figure 5b plots the magnetizations of magnetic molecularly imprinted particles after their absorption of various concentrations of albumin, measured at 15 000 G. It is interesting to note that the

**Table 3. Comparison of Real Sample Measurement by ARCHITECT *ci* 8200 System and the Albumin-Imprinted Magnetic EVAL Composite Nanoparticles**

| | ARCHITECT *ci* 8200 system | MMIPs @ 1500 G | | |
|---|---|---|---|---|
| sample no. | microalbumin (mg/dL) | magnetization (emu/g) | albumin conc. (mg/dL) | accuracy (%) |
| 1 | 0.44 | 7.31 | 0.048 | 10.99 |
| 2 | 0.26 | 4.12 | 0.138 | 53.06 |
| 3 | 0.26 | 2.81 | 0.228 | 87.86 |
| 4 | 0.21 | 2.93 | 0.216 | 97.24 |

**Table 4. Selective Compositions in Real Random Urinary Samples Measured by ARCHITECT *ci* 8200 System[a]**

| sample | microalbumin (mg/dL) | creatinine (mg/dL) | uric acid (mg/dL) | glucos (mg/dL) | urea (mg/dL) | AFP (ng/mL) | CEA (ng/mL) |
|---|---|---|---|---|---|---|---|
| 1 | 0.44 | 98.8 | 40.9 | 4 | 586.44 | <0.4 | 0.55 |
| 2 | 0.26 | 33.7 | 17.1 | 2 | 144.59 | <0.4 | 0.83 |
| 3 | 0.26 | 38.0 | 8.6 | 2 | 162.51 | <0.4 | <0.5 |
| 4 | 0.21 | 30.8 | 8.9 | 2 | 141.56 | <0.4 | <0.5 |

[a] AFP, alpha-fetoprotein; CEA, carcinoembryonic antigen.

decrease in magnetization with increase albumin concentration may in fact be related to the increasing magnitude of surface charge (Figure 4b), which would oppose magnetic-field induced aggregation of the nanoparticles.

Table 3 presents the magnetizations (15 000 G applied) of the magnetic molecularly imprinted particles after the adsorption of real random urine samples, and the interpretation of the magnetization in terms of concentration obtained by applying the calibration curve in Figure 5b. Some magnetizations appear to be inaccurate, as determine by comparison with those measured in hospital using the commercial ARCHITECT *ci* 8200 system at a high concentration of albumin. The interfering compounds in those urine samples are creatinine, uric acid, glucose, urea, AFP, and CEA, whose concentrations are also presented in Table 4. The interference of the albumin-imprinted magnetic EVAL nanoparticles may be caused by either the drying of those particles or interference in the urine. Multiple interferences are found in sample 1, and the concentrations of uric acid and CEA in sample 2 exceed those in samples 3 and 4. Although more real samples may be examined, the usage of liquid sample on a GMR sensor (27), the integration of microelectro-mechanical systems (MEMS), and synthetic receptors may yet achieve higher accuracy in the determination of target molecule concentration by the measurement of superparamagnetic properties (e.g., magnetization). A fuller study of cross-reactivity is planned to investigate the tolerance level to interferences (28) for albumin MMIPs, but is beyond the scope of the present work. At present, we note that the results presented here provide evidence of a significant interference issue in real urine samples, most likely from urea.

To explore the possibility of using MIPs to remove urea, were synthesized magnetic urea-imprinted EVAL nanoparticles using EVAL with 27 mol % ethylene (19c). The mean particles sizes and rebinding capacity in a batch adsorption

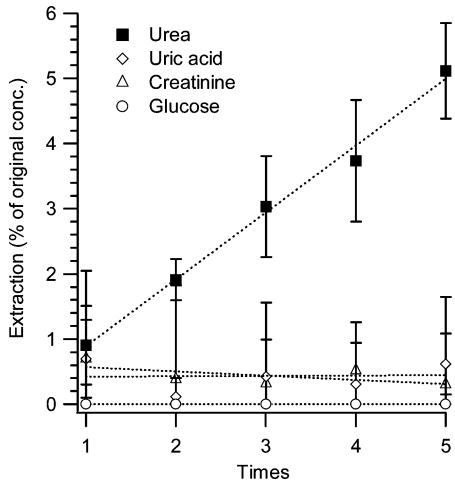


**FIGURE 6. Continuous extraction of urine samples with the magnetic urea-imprinted EVAL nanoparticles. The extraction efficiency is presented in the percentage removed.**

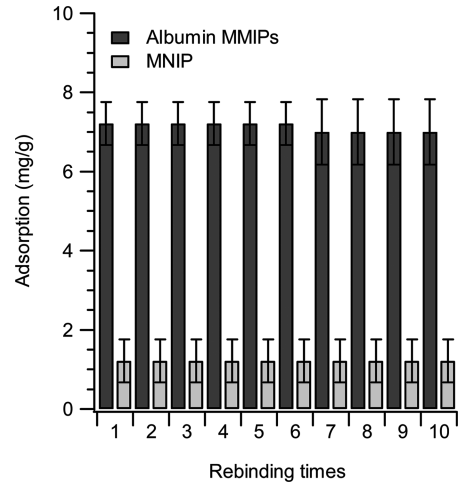


**FIGURE 7. Rebinding stability of the albumin MMIPs examined after storage in a dehumidifier (freeze-dried) for more than 1 year (ca. 14 months).**

are around 56 ± 1 nm and 25.86 ± 0.23 mg/g (in 10 mg/mL urea solution), respectively. In Figure 6, 1 mL of each of five stock urine samples was repeatedly extracted with 15 mg of the magnetic urea-imprinted EVAL nanoparticles. For smaller control (nontarget) molecules (glucose, uric acid and creatinine), the total amount removed after five extractions is less than 1% of the original concentration. Notably, the original concentration of those smaller molecules in urine can be found in Table 4 and are all lower than urea. The adsorption amounts of those interferences on the magnetic urea-imprinted EVAL nanoparticles are likely to be very low. The overall removal of urea from urine steadily increased to 5.12 ± 0.73% after five extractions; each extraction removed 1.04 ± 0.77% of urea in the 25 magnetic extractions processes. When using MNIPs for the removal of urea from urine samples, the average adsorption is 0 within uncertainty 0.54% in 12 magnetic extractions processes.

The stability of albumin MMIPs were tested by measuring their adsorption capacity (30 min adsorption) using the MMIPs are freezing dried and stored in a dehumidifier for 14 months. As shown in Figure 7, there is only a slight decrease in the adsorption capacity (<3% of the first time usage) after six continuous adsorption and washing processes.

## 4. CONCLUSIONS

Poly(ethylene-*co*-ethylene alcohol) not only has the advantage of being biocompatible for the latter in vivo applications but also can easily undergo polymer processing for molecular imprinting. In this study, the synthesis of magnetic molecularly imprinted EVAL nanoparticles with creatinine, albumin, and lysozyme was demonstrated and those target molecules were rapidly adsorbed (~1 min), though optimal absorption of albumin required ~30 min. MIPs with magnetic nanoparticles incorporated (magnetic MIPs, or MMIPs) showed changes in their magnetization in response to rebinding, indicating that magnetization may be a useful readout for MMIP binding and thus target concentrations. MMIP nanoparticles may be able to be integrated into GMR sensors for biosensing applications. Finally, preliminary studies using real urine samples showed promise for magnetic sensing of albumin concentration, but also demonstrated that interferences from other molecular species in urine must be more fully quantified, or interfering species must be removed.

**Acknowledgment.** We appreciate financial supports from National Science Council of ROC under Contract NSC 98-2220-E-390-002.

## REFERENCES AND NOTES

(1) Gupta, A. K.; Gupta, M. *Biomaterials* **2005**, *26*, 3995.
(2) Hong, R. Y.; Feng, B.; Chen, L. L.; Liu, G. H.; Li, H. Z.; Zheng, Y.; Wei, D. G. *Biochem. Eng. J.* **2008**, *42*, 290.
(3) (a) Hillberg, A. L.; Brain, K. R.; Allender, C. J. *Adv. Drug Delivery Rev.* **2005**, *57*, 1875. (b) Haupt, K.; Belmont, A.-S. Molecularly Imprinted Polymers as Recognition Elements in Sensors. In *Handbook of Biosensors and Biochips*; Marks, R. S., Lowe, C. R., Cullen, D. C., Weetall, H. H., Karube, I., Eds.; John Wiley & Sons: Hoboken, NJ, 2008. (c) Danielsson, B. In *Biosensing for the 21st Century*; Renneberg, R., Lisdat, F., Eds.; Advances in Biochemical Engineering Biotechnology; Springer: New York, 2008; Vol. 109.
(4) (a) Wu, Z.; Tao, C.-a.; Lin, C.; Shen, D.; Li, G. *Chem.—Eur. J.* **2008**, *14*, 11358. (b) Otero-Roman, J.; Moreda-Piñeiro, A.; Bermejo-Barrera, P.; Martin-Esteban, A. *Talanta* **2009**, *79*, 723. (c) Ng, S. M.; Narayanaswamy, R. *Sens. Actuators, B* **2009**, *139*, 156. (d) Lieberzeit, P. A.; Dickert, F. L. *Anal. Bioanal. Chem.* **2008**, *391*, 1629. (e) Henry, O. Y. F.; Cullen, D. C.; Piletsky, S. A. *Anal. Bioanal. Chem.* **2005**, *382*, 947. (f) Chen, Y.-C.; Brazier, J. J.; Yan, M.; Bargo, P. R.; Prahl, S. A. *Sens. Actuators, B* **2004**, *102*, 107.
(5) (a) Jenik, M.; Schirhagl, R.; Schirk, C.; Hayden, O.; Lieberzeit, P.; Blaas, D.; Paul, G.; Dickert, F. L. *Anal. Chem.* **2009**, *81*, 5320. (b) Dickert, F. L.; Hayden, O.; Lieberzeit, P.; Haderspoeck, C.; Bindeus, R.; Palfinger, C.; Wirl, B. *Synth. Met.* **2003**, *138*, 65. (c) Dickert, F.; Hayden, O.; Bindeus, R.; Mann, K.-J.; Blaas, D.; Waigmann, E. *Anal. Bioanal. Chem.* **2004**, *378*, 1929. (d) Avila, M.; Zougagh, M.; Ríos, Á.; Escarpa, A. *TrAC, Trends Anal. Chem.* **2008**, *27*, 54.
(6) (a) Kempe, M.; Mosbach, K. *J. Chromatogr., A* **1995**, *691*, 317. (b) Guo, T. Y.; Xia, Y. Q.; Hao, G. J.; Song, M. D.; Zhang, B. H. *Biomaterials* **2004**, *25*, 5905. (c) Chen, L.; Liu, J.; Zeng, Q.; Wang, H.; Yu, A.; Zhang, H.; Ding, L. *J. Chromatogr., A* **2009**, *1216*, 3710.
(7) Ansell, R. J. *Adv. Drug Delivery Rev.* **2005**, *57*, 1809.
(8) (a) Byrne, M. E.; Park, K.; Peppas, N. A. *Adv. Drug Delivery Rev.* **2002**, *54*, 149. (b) Mayes, A. G.; Whitcombe, M. J. *Adv. Drug Delivery Rev.* **2005**, *57*, 1742. (c) Bayer, C. L.; Peppas, N. A. *J. Controlled Release* **2008**, *132*, 216. (d) Caldorera-Moore, M.; Peppas, N. A. *Adv. Drug Delivery Rev.* **2009**, *61*, 1391.
(9) Bergmann, N. M.; Peppas, N. A. *Prog. Polym. Sci.* **2008**, *33*, 271.
(10) Ansell, R. J.; Mosbach, K. *Analyst* **1998**, *123*, 1611.
(11) Lu, S.; Cheng, G.; Zhang, H.; Pang, X. *J. Appl. Polym. Sci.* **2006**, *99*, 3241.

(12) Lu, S.; Cheng, G.; Pang, X. *J. Appl. Polym. Sci.* **2003**, *89*, 3790.
(13) Hu, Y.; Liu, R.; Zhang, Y.; Li, G. *Talanta* **2009**, *79*, 576.
(14) Candan, N.; T men, N.; Andac, M.; Andac, C. A.; Say, R.; Denizli, A. *Mater. Sci. Eng., C* **2009**, *29*, 144.
(15) (a) Ren, Y.; Zhang, M.; Zhao, D. *Desalination* **2008**, *228*, 135. (b) Ren, Y.; Wei, X.; Zhang, M. *J. Hazard. Mater.* **2008**, *158*, 14.
(16) Wang, X.; Wang, L.; He, X.; Zhang, Y.; Chen, L. *Talanta* **2009**, *78*, 327.
(17) Cheng, L.-P.; Lin, H.-Y.; Chen, L.-W.; Young, T.-H. *Polymer* **1998**, *39*, 2135.
(18) Silvestri, D.; Coluccio, M. L.; Barbani, N.; Ciardelli, G.; Cristallini, C.; Pegoraro, C.; Giusti, P. *Desalination* **2006**, *199*, 138.
(19) (a) Lee, M.-H.; Thomas, J. L.; Tasi, S.-B.; Liu, B.-D.; Lin, H.-Y. *J. Nanosci. Nanotechnol.* **2009**, *9*, 3469. (b) Lee, M.-H.; Tsai, T.-C.; Thomas, J. L.; Lin, H.-Y. *Desalination* **2008**, *234*, 126. (c) Huang, C.-Y.; Tsai, T.-C.; Thomas, J. L.; Lee, M.-H.; Liu, B.-D.; Lin, H.-Y. *Biosens. Bioelectron.* **2009**, *24*, 2611.
(20) Lin, H.-Y.; Hsu, C.-Y.; Thomas, J. L.; Wang, S.-E.; Chen, H.-C.; Chou, T.-C. *Biosens. Bioelectron.* **2006**, *22*, 534.
(21) Goldsby, R. A.; Kindt, T. J.; Osborne, B. A.; Kuby, J. *Immunology*; W. H. Freeman and Company: New York, 2003.
(22) Young, T. H.; Cheng, L. P.; Hsieh, C. C.; Chen, L. W. *Macromolecules* **1998**, *31*, 1229.
(23) Pegoraro, C.; Silvestri, D.; Ciardelli, G.; Cristallini, C.; Barbani, N. *Biosens. Bioelectron.* **2008**, *24*, 748.
(24) Umpleby, R. J.; Baxter, S. C.; Bode, M.; Berch, J. K.; Shah, R. N.; Shimizu, K. D. *Anal. Chim. Acta* **2001**, *435*, 35.
(25) (a) Corton, E.; García-Calzón, J. A.; Díaz-García, M. E. *J. Non-Cryst. Solids* **2007**, *353*, 974. (b) Medina-Castillo, A. L.; Mistlberger, G. n.; Fernandez-Sanchez, J. F.; Segura-Carretero, A.; Klimant, I.; Fernandez-Gutierrez, A. *Macromolecules* **2009**, *43*, 55.
(26) García-Calzón, J. A.; Díaz-García, M. E. *Sens. Actuators, B* **2007**, *123*, 1180.
(27) Rife, J. C.; Miller, M. M.; Sheehan, P. E.; Tamanaha, C. R.; Tondra, M.; Whitman, L. J. *Sens. Actuators, A* **2003**, *107*, 209.
(28) Campaña, A. M. G.; Rodríguez, L. C.; Linares, C. J.; Barrero, F. A.; Ceba, M. R. *Anal. Lett.* **1995**, *28*, 369.

AM100227R